Fig. 2. Inhibition of TAK1 Activation in HeLa Cells.

A, Western blot analysis of phosphorylation of NF-κB signaling proteins. HeLa cells were treated with and without EPQB for 2 h and stimulated with 20 ng/ml of TNF-α for 5 min. p-TAK1, p-IKKβ, and p-I-κB indicate phosphorylated molecules. B, Polyubiquitination of RIP. HEK293T cells were stimulated with or without TNF-α for 5 min. Samples were immunoprecipitated with anti-RIP antibody and analyzed by Western blot. The asterisk denotes the heavy chain band, and # indicates a nonspecific band. C, *In vitro* TAK1 kinase assay. Human recombinant TAK1-TAB1 protein was incubated with and without EPQB, and was subjected to kinase reactions with MKK6 and γ-[³²P] ATP. The percentage of kinase inhibition was quantified with a bioimage analyzer.

ylated MKK6, but EPQB inhibited TAK1 kinase activity in a dose-dependent manner (Fig. 2C). These results suggest that EPQB directly inhibits TAK1 activity in NF-κB signaling.

EPQB covalently binds TAK1-TAB1 fusion protein

Because EPQB directly inhibits TAK1 kinase activity, we anticipated that EPQB would bind to TAK1. To investigate this possibility, we tested the binding of EPQB to a recombinant TAK1-TAB1 fusion protein using Bio-EPQB. As shown in Fig. 3A, Bio-EPQB covalently bound to the TAK1-TAB1 fusion protein, and its binding was precluded by EPQB in a dose-dependent manner. The binding between TAK1-TAB2 fusion protein and Bio-EPQB was inhibited by cysteine and glutathione, but not by serine (Supplemental Fig. 3; see *Biosci. Biotechnol. Biochem.* Web site). These results suggest that EPQB covalently binds to TAK1-TAB1/2 complex through cysteine residues.

EPQB crosslinks TAK1 and inhibits NF-κB signaling

When EPQB was administered to Flag-tagged TAK1-overexpressed cells, we noticed that several hypershifted bands appeared in an EPQB-dependent manner (Fig. 3B the left panel). Because these proteins did not represent polyubiquitinated bands (Supplemental Fig. 4; see *Biosci. Biotechnol. Biochem.* Web site), this result suggests that Flag-tagged TAK1 was covalently incorporated into

high-molecular weight complexes. Furthermore, treatment of recombinant TAK1-TAB1 with EPQB also elicited the formation of ladder-like hypershifted variants of TAK1-TAB1 protein *in vitro* (Fig. 3B the right panel); the apparent molecular weights of these newly appearing proteins were 90, 120–140, and 170–200 kDa, as observed by SDS–PAGE. Because recombinant TAK1-TAB1 fusion protein weighs only 45 kDa, these results strongly suggest that EPQB induces covalent crosslinking between TAK1 and other proteins.

To exclude the possibility that NF-κB signaling is inhibited only by cysteine modification and not by crosslinking, we treated cells with *N*-ethylmaleimide (NEM), a nonspecific and cell-permeable thiol binder. NEM did not inhibit TAK1 phosphorylation, suggesting that cysteine residues are not involved in TAK1 activation (Supplemental Fig. 5; see *Biosci. Biotechnol. Biochem.* Web site).

Before stimulation with EPQB and TNF-α, Flag-tagged TAK1-overexpressed cells were treated with and without NEM to block the cysteine residues that bind to EPQB. Then TAK1 proteins were immunoprecipitated and analyzed by Western blot. As shown in Fig. 3C, TAK1 crosslinking was inhibited by NEM pretreatment, suggesting that NEM modified the cysteine residues targeted by EPQB. Under this condition, EPQB failed to inhibit the phosphorylation of TAK1, suggesting that modification of the cysteine residues alone is insufficient
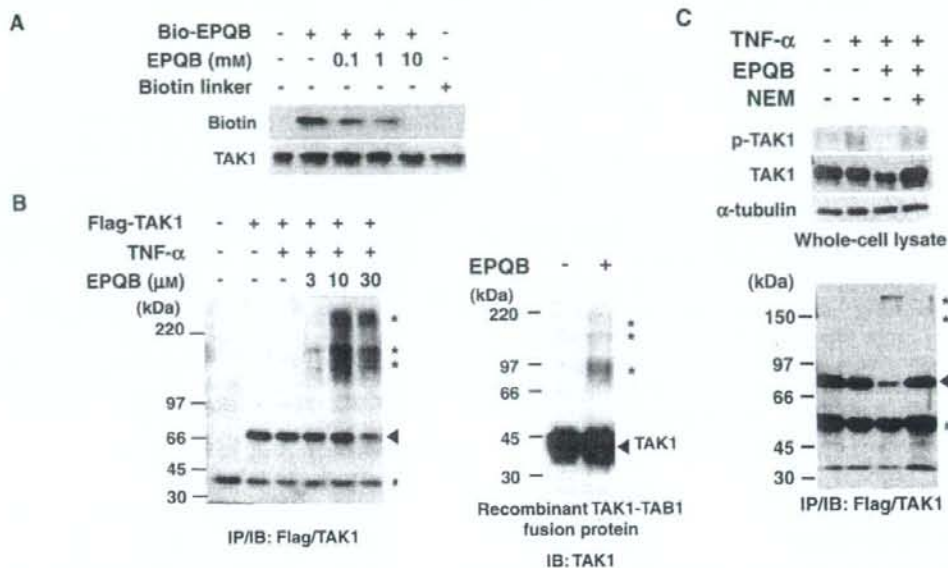
Fig. 3. EPQB Covalently Binds and Crosslinks TAK1 Proteins.
A, Binding assay between EPQB and TAK1. Recombinant TAK1-TAB1 fusion protein was pretreated with and without EPQB at various concentrations for 1 h as the competitor, and then incubated with Bio-EPQB at 0.5 mM for 1 h at 37 °C. The samples were analyzed by Western blot. B, Appearance of supershifted bands containing TAK1 under EPQB treatment. Flag-TAK1-overexpressing HeLa cells were treated with EPQB at various concentrations for 2 h. The samples were immunoprecipitated with anti-Flag antibody (left panel). Recombinant TAK1-TAB1 fusion protein (45 kDa) was treated with EPQB at 10 mM for 2 h in vitro (right panel). These samples were analyzed by Western blot. C, Flag-TAK1-overexpressing HeLa cells were pretreated with N-ethylmaleimide for 1 h at 300 μM and treated with EPQB at 30 μM for 1 h. These samples were immunoprecipitated with anti-Flag antibody and analyzed by Western blot. The asterisk denotes a supershifted band, and # indicates a nonspecific band. The arrow head indicates TAK1 protein band (77 kDa).

for TAK1 inhibition. Instead, crosslinking of EPQB to TAK1 or to TAK1 and other proteins appears to be critical to EPQB-mediated inhibition.

Discussion

NF-κB activation occurs in rheumatoid arthritis, kidney inflammation, and malignant tumor growth.[15-17] Hence, pharmaceutical inhibitors of NF-κB activation have been screened and developed as potential therapeutic agents. Because Cys179 of IKKβ has been reported to be the target of several fungus-derived epoxyquinoids,[4-6] we examined the effects of EPQB on NF-κB signaling by cDNA microarray.

We found that EPQB inhibited the expression of TNF-α-induced genes, such as NF-κB, I-κB, ICAM1, VCAM1, and E-selectin (Fig. 1B). In addition, it significantly inhibited nuclear translocation of NF-κB and TAK1 phosphorylation at Thr187 (Fig. 2A). Because phosphorylation of TAK1 at Thr187 is crucial to IKK activation and subsequently to NF-κB,[12] we focused on the inhibition of TAK1 activation by EPQB.

TAK1 is one of the most well-characterized mitogen-activated protein kinase kinase kinases, and the binding of polyubiquitinated RIP via the TAB2 zinc finger domain is necessary to TAK1 activation.[18,19] Hence we

examined to determine whether TAK1 kinase activity and RIP polyubiquitination would be inhibited by EPQB.

Immunoprecipitation analysis revealed that EPQB did not inhibit RIP polyubiquitination (Fig. 2B). Furthermore, EPQB inhibited the kinase activity of the TAK1-TAB1 fusion protein in a dose-dependent manner (Fig. 2C). These results strongly suggest that EPQB inhibits TAK1 activity directly in the context of TNF-α-induced NF-κB signaling.

Although TAK1 plays a critical role in the activation of NF-κB signaling, few inhibitors of TAK1 have been reported. 5Z-7-oxozeaenol, a resorcylic lactone of fungal origin, inhibits the interleukin-induced activation of TAK1, IKK, JNK, p38, and NF-κB in vitro and shows anti-inflammatory activity in vivo.[20] This report also suggests that a TAK1 inhibitor is a potential candidate for the inhibitor of NF-κB signaling.

In this study, we found that EPQB covalently bound recombinant TAK1-TAB1 fusion protein (Fig. 3A) and, that EPQB induced crosslinking to TAK1 itself, or to TAK1 and other proteins, which might cause inhibition of NF-κB signaling (Fig. 3B, C). We reported recently that EPQB showed anti-angiogenic effects, and covalently bound to two cysteines.[8] Furthermore, we found that EPQB crosslinked through cysteine residues on

recombinant VEGFR2 kinase protein in an EPQB-dependent manner.[9] These results suggest that EPQB has multiple targets, and that the crosslinking of target proteins induces inhibition of several signal transductions. There are a few reports that compounds crosslink two cysteines of target proteins. Guido *et al.* has suggested that helenalin, a sesquiterpene lactone, crosslinks proteins through cysteine residues on NF-κB.[21] Because the active site of NF-κB contains several cysteine residues, helenalin might affect NF-κB signaling by binding and crosslinking to it. The kinase activation loop of TAK1, which contains an autophosphorylation site at threonine residues (Thr184 and Thr187) and a serine residue (Ser192), also contains a cysteine residue (Cys180).[22] Therefore, we propose that EPQB inhibits NF-κB signaling through EPQB-induced crosslinking with TAK1 and other proteins.

In this study, we found that EPQB inhibits TNF-α-induced TAK1 activity by crosslinking to TAK1 itself or to TAK1 and other proteins. These results strongly suggest that the mechanism of inhibition of EPQB differs from that of other epoxyquinoids, because EPQB harbors a highly reactive element that contains two epoxides. Hence, EPQB might be a good lead compound to design a crosslinking agent to prevent signal transduction.

Acknowledgment

References

1) Bremner, P., and Heinrich, M., Natural products as targeted modulators of the nuclear factor-κB pathway. *J. Pharm. Pharmacol.*, **54**, 453–472 (2002).

2) Ariga, A., Namekawa, J., Matsumoto, N., Inoue, J., and Umezawa, K., Inhibition of tumor necrosis factor-α-induced nuclear translocation and activation of NF-κB by dehydroxymethylepoxyquinomicin. *J. Biol. Chem.*, **277**, 24625–24630 (2002).

3) Liang, M., Bardhan, S., Li, C., Pace, E. A., Porco, J. A., Jr., and Gilmore, T. D., Jesterone dimer, a synthetic derivative of the fungal metabolite jesterone, blocks activation of transcription factor nuclear factor κB by inhibiting the inhibitor of κB kinase. *Mol. Pharmacol.*, **64**, 123–131 (2003).

4) Kwok, B. H., Koh, B., Ndubuisi, M. I., Elofsson, M., and Crews, C. M., The anti-inflammatory natural product parthenolide from the medical herb *feverfew* directly binds to and inhibits IκB kinase. *Chem. Biol.*, **8**, 759–766 (2001).

5) Bernier, M., Kwon, Y. K., Pandey, S. K., Zhu, T. N.,

Zhao, R. J., Maciuk, A., He, H. J., DeCabo, R., and Kole, S., Binding of manumycin A inhibits IκB kinase β activity. *J. Biol. Chem.*, **281**, 2551–2561 (2006).

6) Liang, M., Bardhan, S., Pace, E. M., Rosman, D., Beutler, J. A., Porco, J. A., Jr., and Gilmore, T. D., Inhibition of transcription factor NF-κB signaling proteins IKKβ and p65 through specific cysteine residues by epoxyquinone A monomer: correlation with its anti-cancer cell growth activity. *Biochem. Pharmacol.*, **71**, 634–645 (2006).

7) Byun, M. S., Choi, J., and Jue, D. M., Cysteine-179 of IkappaB kinase beta plays a critical role in enzyme activation by promoting phosphorylation of activation loop serines. *Exp. Mol. Med.*, **38**, 546–552 (2006).

8) Kamiyama, H., Kakeya, H., Usui, T., Nishikawa, K., Shoji, M., Hayashi, Y., and Osada, H., Epoxyquinol B shows antiangiogenic and antitumor effects by inhibiting VEGFR2, EGFR, FGFR, and PDGFR. *Oncol. Res.*, **17**, 11–21 (2008).

9) Kamiyama, H., Usui, T., Uramoto, M., Takagi, H., Shoji, M., Hayashi, Y., Kakeya, H., and Osada, H., A fungal metabolite, Epoxyquinol B, crosslinks proteins by epoxy-thiol conjugation. *J. Antibiotics*, **61**, 94–97 (2008).

10) Shoji, M., Yamaguchi, J., Kakeya, H., Osada, H., and Hayashi, Y., Total synthesis of (+)-epoxyquinols A and B. *Angew. Chem. Int. Ed. Engl.*, **41**, 3192–3194 (2002).

11) Sakurai, H., Miyoshi, H., Toriumi, W., and Sugita, T., Functional interactions of transforming growth factor beta-activated kinase 1 with IkappaB kinases to stimulate NF-κB activation. *J. Biol. Chem.*, **274**, 10641–10648 (1999).

12) Singhirunnusorn, P., Suzuki, S., Kawasaki, N., Saiki, I., and Sakurai, H., Critical roles of threonine 187 phosphorylation in cellular stress induced rapid and transient activation of transforming growth factor-β-activated kinase 1 (TAK1) in a signaling complex containing TAK1-binding protein TAB1 and TAB2. *J. Biol. Chem.*, **280**, 7359–7368 (2005).

13) Chen, Z. J., Ubiquitin signaling in the NF-κB pathway. *Nat. Cell Biol.*, **8**, 758–765 (2005).

14) Kanayama, A., Seth, R. B., Sun, L., Ea, C. K., Hong, M., Shaito, A., Chiu, Y. H., Deng, L., and Chen, Z. J., TAB2 and TAB3 activate the NF-κB pathway through binding to polyubiquitin chains. *Mol. Cell*, **15**, 535–548 (2004).

15) Hoffmann, J. A., Kafatos, F. C., Janeway, C. A., and Ezekowitz, R. A. B., Phylogenetic perspectives in innate immunity. *Science*, **284**, 1313–1318 (1999).

16) Ghosh, S., May, M. J., and Kopp, E. B., NF-κB and REL proteins: evolutionary conserved mediators of immune responses. *Annu. Rev. Immunol.*, **16**, 225–260 (1998).

17) Calzado, M. A., Bacher, S., and Schmitz, M. L., NF-κB inhibitors for the treatment of inflammatory diseases and cancer. *Curr. Med. Chem.*, **14**, 367–376 (2007).

18) Shirakabe, K., Yamaguchi, K., Shibuya, H., Irie, K., Matsuda, S., Moriguchi, T., Gotoh, Y., Matsumoto, K., and Nishida, E., TAK1 mediates the ceramide signaling to stress-activated protein kinase/c-Jun N-terminal kinase. *J. Biol. Chem.*, **272**, 8141–8144 (1997).

19) Ninomiya-Tsuji, J., Kishimoto, K., Hiyama, A., Inoue, J., Cao, Z., and Matsumoto, K., The kinase TAK1 can activate the NIK-I κ B as well as the MAP kinase cascade in the IL-1 signaling pathway. *Nature*, **398**,

252–256 (1999).

20) Ninomiya-Tsuji, J., Kajino, T., Ono, K., Ohtomo, T., Matsumoto, M., Shiina, M., Mihara, M., Tsuchiya, M., and Matsumoto, K., A resorcylic acid lactone, 5Z-7-oxozeaenol, prevents inflammation by inhibiting the catalytic activity of TAK1 MAPK kinase. *J. Biol. Chem.*, **278**, 18485–18490 (2003).

21) Guido, L., Knorre, A., Schmidt, T. J., Pahl, H. L., and Merfort, I., The anti-inflammatory sesquiterpene lactone helenalin inhibits the transcription factor NF-κB by directly targeting p65. *J. Biol. Chem.*, **273**, 33508–33516 (1998).

22) Brown, K. B., Vial, S. C., Dedi, N., Long, J. M., Dunster, N. J., and Cheetham, G. M. T., Structural basis for the interaction of TAK1 kinase with its activating protein TAB1. *J. Mol. Biol.*, **354**, 1013–1020 (2005).

Natural Product Synthesis

The Asymmetric Total Synthesis of (+)-Cytotrienin A, an Ansamycin-Type Anticancer Drug[**]

Yujiro Hayashi, Mitsuru Shoji, Hayato Ishikawa, Junichiro Yamaguchi, Tomohiro Tamura, Hiroki Imai, Yosuke Nishigaya, Kenichi Takabe, Hideaki Kakeya, and Hiroyuki Osada*

Cytotrienin A (**1**) is a microbial antitumor secondary metabolite that was isolated from the fermentation broth of *Streptomyces sp.* RK95-74 from soil.[1] It possesses an
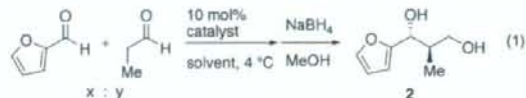

(+)-cytotrienin A (**1**)
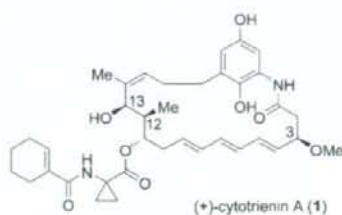
E,E,E-triene motif within a 21-membered cyclic lactam, which also contains four chiral centers. These are common structural features of the ansamycin class of natural products, which include the mycotrienins (or ansatrienins),[2] trienomycins,[2c,3] thiazinotrienomycins,[4] and trierixin.[5] Cytotrienin A, with its unusual aminocyclopropane carboxylic acid side chain, exhibits potent apoptosis-inducing activity on HL-60 cells with an ED_{50} value of 7.7 nM. To facilitate elucidation of its mechanism of action, the development of a method for the total synthesis and derivatization of cytotrienin A is highly desirable. The research groups of Smith and Panek have
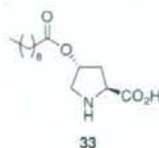
accomplished the total synthesis of other members of this class of natural products, including trienomycins A and F,[6] mycotrienin A,[7] and thiazinotrienomycin E.[8] Although the macrocyclic core of cytotrienin A has been synthesized in its protected form by Panek et al.[9] and Kirschning et al.,[10] the total synthesis of cytotrienin A, with the side chain attached, has not been reported. The relative and absolute stereochemistry has not been confirmed, but has been assigned based on analogous mycotrienin natural products. Herein we report the first total synthesis of the naturally occurring enantiomer of cytotrienin A, which confirms its relative and absolute stereochemistry.

We envisioned installing the side chain midway through the synthesis and constructing the triene unit at a late stage by ring-closing metathesis (RCM).[11] We reasoned that introduction of the bulky side chain after formation of the macrocyclic core would be difficult, and also, a long sequence of reactions after the construction of the labile triene unit would be avoided. Other noteworthy features of our approach are the use of novel organocatalyzed and proline-mediated enantioselective reactions, both of which have been developed by our research group.[12] Specifically, we planned to form two (C11 and C12) of the three contiguous chiral centers with an aldol reaction by using an organocatalyst, and to control the configuration at C3 by using proline-mediated α-aminoxylation.

The synthesis started with an organocatalyzed aldol reaction which was found to be problematic. The original procedure[13] which used proline was not practical for large-scale synthesis owing to the excess amount of furfural required (10 equivalents), low yield, and low diastereoselectivity [Eq. (1)]. After some experimentation, diol **2** was obtained in good yield and with good d.e. when the reaction was conducted without solvent using surfactant-proline con-

[*] Prof. Dr. Y. Hayashi, Dr. M. Shoji,[+] Dr. H. Ishikawa, J. Yamaguchi,
T. Tamura, H. Imai, Y. Nishigaya, K. Takabe
Department of Industrial Chemistry, Faculty of Engineering
Tokyo University of Science, Kagurazaka, Shinjuku-ku, Tokyo 162-8601 (Japan)
Fax: (+81) 3-5261-4631
E-mail: hayashi@ci.kagu.tus.ac.jp
Homepage: http://www.ci.kagu.tus.ac.jp/lab/org-chem1/

Prof. Dr. H. Kakeya
Graduate School of Pharmaceutical Sciences
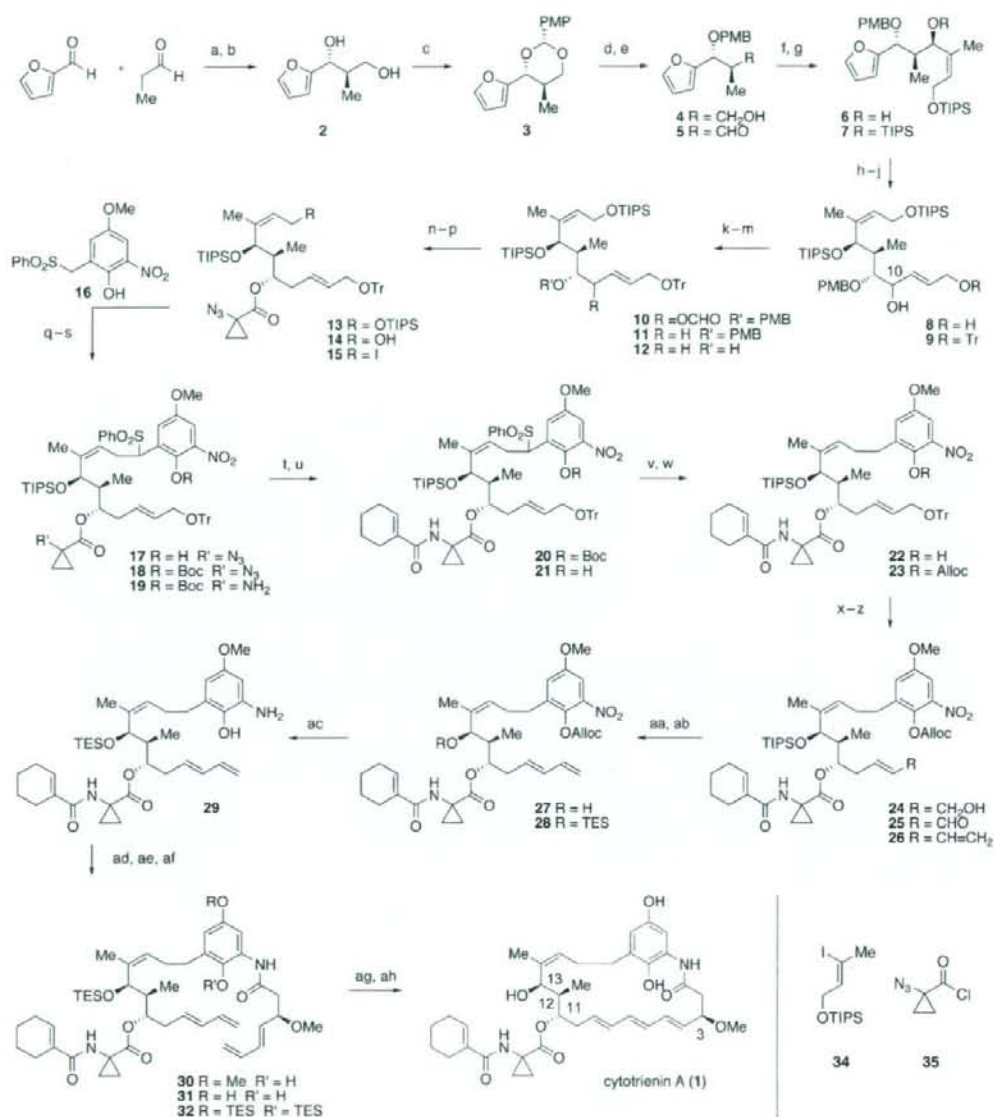Kyoto University, Sakyo-ku, Kyoto-city, Kyoto 606-8501 (Japan)

Prof. Dr. H. Osada
Antibiotics Laboratory
RIKEN Discovery Research Institute
Wako, Saitama 351-0198 (Japan)

[+] Present address:
Department of Chemistry, Graduate School of Science
Tohoku University, Sendai 980-8578 (Japan)

proline x/y = 10:1 DMF   32 h 10% anti/syn = 1:1
cat. **33** x/y = 1:5 neat 48 h 77% anti/syn = 6.2:1, 96% ee


33

Communications

Scheme 1. Reagents and conditions: a) **33**, 4°C, 48 h; b) NaBH₄, MeOH, 0°C, 1 h (77%, 96% *ee*, *anti:syn* 6.2:1); c) *p*-MeOPhCH(OMe)₂, PPTS, benzene, 80°C, 1 h (64%, >99% *ee* after recrystallization); d) DIBAL-H, Et₂O, −78°C to −10°C, 128 h [80% (92% brsm)]; e) SO₃·py, DMSO, Et₃N, CH₂Cl₂, 0°C, 45 min (quant.); f) **34**, *t*BuLi, THF, −78°C, 1 h; Me₂Zn, 0°C, 20 min; then **5** at −78°C; −35°C, 3 h (79%); g) TIPSOTf, 2,6-lutidine, CH₂Cl₂, 0°C, 23 h (99%); h) O₂, Rose Bengal, EtCN, *hv*, −78°C, 8 h; Me₂S, −20°C, 15 h; DABCO, −20°C, 2 h; i) NaBH₄, CeCl₃·7H₂O, EtOH, 0°C, 20 min (81% from **7**); j) TrCl, Et₃N, CH₂Cl₂, 23°C, 3 h (93%); k) 1*H*-benzotriazole-1-carbaldehyde, DMAP, CH₂Cl₂, 23°C, 4 h (quant.); l) [Pd₂(dba)₃]·CHCl₃, *n*Bu₃P, HCO₂NH₄, 1,4-dioxane, 23°C, 67 h (76%); m) DDQ, CH₂Cl₂/pH 7 phosphate buffer, 0°C, 4 h (96%); n) **35**, DMAP, Et₃N, 0°C, 20 min (98%); o) py(HF)ₓ, THF, 23°C, 17 h (84%); p) I₂, Ph₃P, imidazole, benzene, 23°C, 30 min; q) **16**, LHMDS, THF, −90°C, 40 min; then **15** at −90°C; −65°C, 18 h (78% from **14**); r) (Boc)₂O, DMAP, CH₂Cl₂, 23°C, 30 min (96%); s) 1,3-propanedithiol, Et₃N, MeOH, 23°C, 18 h (87%); t) 1-cyclohexenecarboxylic acid, EDCI, DMAP, CH₂Cl₂, 23°C, 21 h (78%); u) pyrrolidine, CH₂Cl₂, 23°C, 5 h; v) NaBH₄, EtOH, 50°C, 21 h (57% from **20**); w) AllocCl, Et₃N, CH₂Cl₂, 23°C, 40 min; x) TsOH·H₂O, MeOH, 23°C, 1 h (94% from **22**); y) MnO₂, CH₂Cl₂, 23°C, 40 min; z) [Ph₃P⁺CH₃]I⁻, *t*BuOK, THF, 0°C, 30 min (74% from **24**); aa) 46% HF, MeCN, 23°C, 16 h [68% (91% brsm)]; ab) TESOTf, *i*Pr₂EtN, CH₂Cl₂, 23°C, 30 min (99%); ac) NaBH₄, Sₓ, THF, 23°C, 2.5 h; ad) **42**, BOP-Cl, *i*Pr₂EtN, toluene, 23°C, 8 h; K₂CO₃, MeOH, 23°C, 10 min (79% from **28**); ae) MnO₂, CH₂Cl₂, 23°C, 5 min; NaBH₄, MeOH, 0°C; af) 4-triethylsiloxy-3-penten-2-one, DMF, 23°C to 50°C, 9 h (77% from **30**); ag) Grubbs I catalyst (40 mol%), CH₂Cl₂, 23°C, 71 h [39% (51% brsm)]; ah) Amberlyst 15, THF/H₂O (10:1), 23°C, 47 h (95%). Definitions of acronyms given in reference [28].

jugated catalyst **33**.[14] This catalyst was developed by us for aldol reactions in the presence of water. As this reaction proceeds without solvent, scale-up and purification are straightforward. Diol **2** was treated with *p*-anisaldehyde dimethyl acetal in the presence of PPTS to provide **3**, which was isolated in diastereomerically and optically pure form (> 99 % *ee*) after recrystallization (and without the need for column chromatography; Scheme 1).

Reduction of **3** with DIBAL-H gave primary alcohol **4** in 80 % yield (92 % yield based on recovered starting material (brsm)). Alcohol **4** was oxidized to aldehyde **5** quantitatively. The reaction of **5** with vinyl zincate,[15] prepared from vinyl iodide **34** with *t*BuLi and Me₂Zn, proceeded in a highly diastereoselective manner to afford **6** as a single isomer in 79 % yield. Notably, other vinyl metals gave low diastereoselectivities.[16] The secondary hydroxy group of **6** was protected with the TIPS group. The furan ring was cleaved by oxidation with O₂ under irradiation conditions in the presence of Rose Bengal.[17] Subsequent *cis/trans* isomerization using DABCO, followed by Luche reduction[18] gave diol **8** as a mixture of diastereomers at C10 in 81 % yield (over 3 steps). The primary hydroxy group of **8** was protected as the trityl ether. The free hydroxy group of **9** was converted into formate ester **10**, which was removed by reduction using a palladium–PBu₃ complex with the protocol developed by Tsuji and co-workers [19] to provide **11** as a single isomer without positional or *E/Z* isomerization. Removal of the PMB group followed by reaction with acid chloride **35**[20] gave ester **13**. Selective removal of the TIPS group gave primary alcohol **14**, which was transformed into iodide **15** with PPh₃ and I₂. Coupling of fragment **15** and sulfone **16** was successfully performed by the lithiation of hydroxysulfone **16** with LHMDS, followed by alkylation using **15** to afford **17** in 78 % yield (over 2 steps). After protection of the phenol of **17** as its Boc derivative, the azide moiety was reduced to an amine with 1,3-propanedithiol,[21] and the amide bond with cyclohexenyl carboxylic acid was constructed to provide **20** in good yield. This completed installation of the side chain.

Carrying out desulfonylation without affecting the nitro group was difficult. After experimentation, a novel method was developed which consisted of removal of the Boc group with pyrrolidine[22] followed by treatment of phenol **21** with NaBH₄. This method provided **22** in 57 % yield (over 2 steps) through a retro-Michael reaction with SO₂Ph, probably involving *o*-quinonemethide, followed by reduction with NaBH₄. The phenol was protected as its Alloc derivative and removal of the Tr group gave alcohol **24** in 94 % yield (over 2 steps). Oxidation of **24** with MnO₂, followed by a Wittig reaction gave diene **26** in 74 % yield (over 2 steps). As we could not remove the TIPS group after construction of the triene moiety, this protecting group was replaced with the easily removable TES group at this stage. Treatment with HF provided **27** in 91 % yield (brsm), then reaction with TESOTf afforded **28** quantitatively. The nitro group was reduced with NaBH₂S₃[23] and was accompanied by removal the Alloc group to provide **29**. The amine **29** was treated with carboxylic acid **42** (vide infra) in the presence of BOP-Cl to afford **30** in 79 % yield (over 2 steps).

Carboxylic acid **42** was synthesized as shown in Scheme 2. Proline-mediated α-aminoxylation[24] of aldehyde **36** proceeded efficiently to provide **37**. Under Horner–Emmons reaction conditions, a crude sample of **37** was converted into
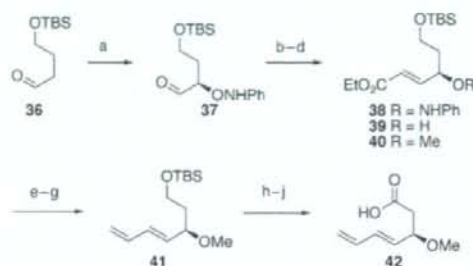
Scheme 2. Reagents and conditions: a) nitrosobenzene, L-proline, MeCN, −20 °C, 24 h; b) triethyl phosphonoacetate, NaH, THF, 23 °C, 45 min; c) CuSO₄, MeOH, 0 °C, 46 h (46 % from **36**, 98 % *ee*); d) MeI, NaH, DMF, 0 °C, 1 h (94 %); e) DIBAL-H, CH₂Cl₂, −78 °C to −40 °C, 2 h; f) MnO₂, CH₂Cl₂, 23 °C, 2 h; g) [Ph₃P⁺CH₃]I⁻, *t*BuOK, THF, 0 °C, 15 min (66 % from **40**); h) py(HF)ₙ, MeCN, 0 °C, 1.5 h; i) SO₃·py, DMSO, Et₃N, CH₂Cl₂, 0 °C, 50 min; j) NaClO₂, NaH₂PO₄·2H₂O, 2-methyl-2-butene, *t*BuOH/H₂O (3:1), 23 °C, 1 h (56 % from **41**).

alcohol **39** by treatment with CuSO₄ in MeOH giving 46 % yield (over 3 steps) with 98 % *ee*. Williamson ether synthesis gave **40** in 94 % yield. Diene **41** was synthesized by a three-step procedure: reduction with DIBAL-H, oxidation with MnO₂, and a Wittig reaction (Ph₃P=CH₂). Carboxylic acid **42** was constructed by removal of the TBS group, oxidation with SO₃·pyridine,[25] and subsequent oxidation by the method of Pinnick and co-workers.[26]

All that remained to complete the synthesis was the crucial ring formation. The protecting group of the phenol was converted from methyl to the more easily removable TES group through an oxidation/reduction sequence: 1) oxidation to the quinone with MnO₂, 2) reduction to hydroquinone **31** with NaBH₄, 3) immediate protection of **31** with 4-triethylsiloxy-3-penten-2-one[27] (this was the best silylating reagent in this particular case as low yields were obtained with other reagents because of the facile oxidation of hydroquinone **31** to quinone by adventitious O₂). Next RCM methodology, which had been used by Panek and co-workers in the synthesis of the core lactam of cytotrienin, was employed.[9] This reaction proceeded slowly when catalyzed by the first-generation Grubbs catalyst to afford triene in 39 % yield along with recovered starting material **32** (23 %), and therefore, a good conversion (51 % brsm) was obtained. Removal of the TES group with Amberlyst 15 gave (+)-cytotrienin A (**1**) in 95 % yield. Synthetic cytotrienin A exhibited spectroscopic properties identical to those of the natural product[1] (¹H NMR and IR spectroscopy, *R*ₜ value, optical rotation, and HPLC analysis) which confirms the absolute stereochemistry.

In summary, the first asymmetric total synthesis of (+)-cytotrienin A has been achieved, and its absolute configuration has been confirmed. There are several noteworthy features to this total synthesis: a practical diastereo- and

Communications

enantioselective aldol reaction using novel catalyst **33** under solvent-free conditions, highly diastereoselective construction of the three contiguous chiral centers, a deoxygenation reaction without positional or *E*/*Z* isomerization (from **10** to **11**), desulfonylation using NaBH$_4$ (from **21** to **22**), control of the absolute configuration at C3 by proline-mediated α-aminoxylation, and RCM for the formation of the 21-membered macrolactam.

[1] a) H. P. Zhang, H. Kakeya, H. Osada, *Tetrahedron Lett.* **1997**, *38*, 1789; b) H. Kakeya, H. P. Zhang, K. Kobinata, R. Onose, C. Onozawa, T. Kudo, H. Osada, *J. Antibiot.* **1997**, *50*, 370; c) H. Osada, H. Kakeya, H. P. Zhang, K. Kobinata, WO 9823594, **1998**; d) H. P. Zhang, H. Kayeka, H. Osada, *Tetrahedron Lett.* **1998**, *39*, 6947; e) H. Kakeya, R. Onose, H. Osada, *Cancer Res.* **1998**, *58*, 4888.

[2] a) M. Sugita, Y. Natori, T. Sasaki, K. Furihata, A. Shimazu, H. Seto, N. Otake, *J. Antibiot.* **1982**, *35*, 1460; b) M. Sugita, T. Sasaki, K. Furihata, A. Shimazu, H. Seto, N. Otake, *J. Antibiot.* **1982**, *35*, 1467; c) A. B. Smith III, J. L. Wood, W. Wong, A. E. Gould, C. J. Rizzo, J. Barbosa, K. Komiyama, S. Omura, *J. Am. Chem. Soc.* **1996**, *118*, 8308.

[3] a) S. Funayama, K. Okada, K. Komiyama, I. Umezawa, *J. Antibiot.* **1985**, *38*, 1107; b) S. Funayama, K. Okada, K. Iwasaki, K. Komiyama, I. Umezawa, *J. Antibiot.* **1985**, *38*, 1677; c) H. Nomoto, S. Katsumata, K. Takahashi, S. Funayama, K. Komiyama, I. Umezawa, S. Omura, *J. Antibiot.* **1989**, *42*, 479.

[4] a) N. Hosokawa, H. Naganawa, H. Inuma, M. Hamada, T. Takeuchi, T. Kanbe, M. Hori, *J. Antibiot.* **1995**, *48*, 471; b) A. B. Smith III, J. Barbosa, N. Hosokawa, H. Naganawa, T. Takeuchi, *Tetrahedron Lett.* **1998**, *39*, 2891.

[5] a) E. Tashiro, N. Hironiwa, M. Kitagawa, Y. Futamura, S. Suzuki, M. Nishio, M. Imoto, *J. Antibiot.* **2007**, *60*, 547; b) Y. Futamura, E. Tashiro, N. Hironiwa, J. Kohno, M. Nishio, K. Shindo, M. Imoto, *J. Antibiot.* **2007**, *60*, 582.

[6] A. B. Smith III, J. Barbosa, W. Wong, J. L. Wood, *J. Am. Chem. Soc.* **1996**, *118*, 8316.

[7] C. E. Masse, M. Yang, J. Solomon, J. S. Panek, *J. Am. Chem. Soc.* **1998**, *120*, 4123.

[8] A. B. Smith III, Z. Wan, *J. Org. Chem.* **2000**, *65*, 3738.

[9] G. Evano, J. V. Schaus, J. S. Panek, *Org. Lett.* **2004**, *6*, 525.

[10] D. Kashin, A. Meyer, R. Wittenberg, K.-U. Schoning, S. Kamlage, A. Kirschning, *Synthesis* **2007**, 304.

[11] Reviews; a) A. Fürstner, *Angew. Chem.* **2000**, *112*, 3140; *Angew. Chem. Int. Ed.* **2000**, *39*, 3012; b) T. M. Trnka, R. H. Grubbs, *Acc.* *Chem. Res.* **2001**, *34*, 18; c) R. H. Grubbs, *Tetrahedron* **2004**, *60*, 7117; d) K. C. Nicolaou, P. G. Bulger, D. Sarlah, *Angew. Chem.* **2005**, *117*, 4564; *Angew. Chem. Int. Ed.* **2005**, *44*, 4490.

[12] Review of total synthesis using organocatalysis; R. Marcia de Figueiredo, M. Christmann, *Eur. J. Org. Chem.* **2007**, 2575.

[13] A. B. Northrup, D. W. C. MacMillan, *J. Am. Chem. Soc.* **2002**, *124*, 6798.

[14] Y. Hayashi, S. Aratake, T. Okano, J. Takahashi, T. Sumiya, M. Shoji, *Angew. Chem.* **2006**, *118*, 5653; *Angew. Chem. Int. Ed.* **2006**, *45*, 5527.

[15] M. Suzuki, Y. Morita, H. Koyano, M. Koga, R. Noyori, *Tetrahedron* **1990**, *46*, 4809.

[16] The corresponding vinyl lithium gave a 1:1 mixture of diastereomers.

[17] C. S. Foote, M. T. Wuesthoff, S. Wexler, I. G. Burstain, R. Denny, G. O. Schenck, K.-H. Schulte-Elte, *Tetrahedron* **1967**, *23*, 2583.

[18] J.-L. Luche, *J. Am. Chem. Soc.* **1978**, *100*, 2226.

[19] a) J. Tsuji, I. Shimizu, I. Minami, *Chem. Lett.* **1984**, 1017; b) J. L. Hubbs, C. H. Heathcock, *J. Am. Chem. Soc.* **2003**, *125*, 12836.

[20] M. C. Pirrung, G. M. McGeehan, *J. Org. Chem.* **1983**, *48*, 5143.

[21] H. Bayley, D. N. Standring, J. R. Knowles, *Tetrahedron Lett.* **1978**, *19*, 3633.

[22] K. Nakamura, T. Nakajima, H. Kayahara, E. Nomura, H. Taniguchi, *Tetrahedron Lett.* **2004**, *45*, 495.

[23] J. M. Lalancette, A. Frehe, J. R. Brindle, M. Laliberté, *Synthesis* **1972**, 526.

[24] a) Y. Hayashi, J. Yamaguchi, K. Hibino, M. Shoji, *Tetrahedron Lett.* **2003**, *44*, 8293; b) Y. Hayashi, J. Yamaguchi, T. Sumiya, M. Shoji, *Angew. Chem.* **2004**, *116*, 1132; *Angew. Chem. Int. Ed.* **2004**, *43*, 1112; c) Y. Hayashi, J. Yamaguchi, T. Sumiya, K. Hibino, M. Shoji, *J. Org. Chem.* **2004**, *69*, 5966; d) G. Zhong, *Angew. Chem.* **2003**, *115*, 4379; *Angew. Chem. Int. Ed.* **2003**, *42*, 4247; e) S. P. Brown, M. P. Brochu, C. J. Sinz, D. W. C. MacMillan, *J. Am. Chem. Soc.* **2003**, *125*, 10808; f) A. Bogevig, H. Sunden, A. Cordova, *Angew. Chem.* **2004**, *116*, 1129; *Angew. Chem. Int. Ed.* **2004**, *43*, 1109.

[25] J. R. Parikh, W. v. E. Doering, *J. Am. Chem. Soc.* **1967**, *89*, 5505;

[26] B. S. Bal, W. E. Childers Jr. , H. W. Pinnick, *Tetrahedron* **1981**, *37*, 2091.

[27] M. Egbertson, S. J. Danishefsky, G. Schulte, *J. Org. Chem.* **1987**, *52*, 4424.

[28] Alloc = allyloxycarbonyl, Boc = *tert*-butyloxycarbonyl, BOP-Cl = bis(2-oxo-3-oxazolidinyl)phosphinic chloride, DABCO = 1,4-diazabicyclo[2.2.2]octane, dba = *trans,trans*-dibenzylideneacetone, DDQ = 2,3-dichloro-5,6-dicyano-1,4-benzoquinone, DIBAL-H = diisobutylaluminum hydride, DMAP = 4-dimethylaminopyridine, DMF = *N,N*-dimethylformamide, DMSO = dimethyl sulfoxide, EDCI = 1-(3-dimethylaminopropyl)-3-ethylcarbodiimide hydrochloride, LHMDS = lithium hexamethyldisilazaide, PPTS = pyridinium *p*-toluenesulfonate, py = pyridine, TES = triethylsilyl, Tf = trifluoromethanesulfonyl, TIPS = triisopropylsilyl, Tr = trityl, Ts = 4-toluenesulfonyl.

ELSEVIER

Synthesis and structure–activity relationship studies on tryprostatin A, an inhibitor of breast cancer resistance protein

Hiteshkumar D. Jain,[a] Chunchun Zhang,[a] Shuo Zhou,[a] Hao Zhou,[a] Jun Ma,[a]
Xiaoxiang Liu,[a] Xuebin Liao,[a] Amy M. Deveau,[a] Christine M. Dieckhaus,[b]
Michael A. Johnson,[b] Kirsten S. Smith,[b] Timothy L. Macdonald,[b]
Hideaki Kakeya,[c] Hiroyuki Osada[c] and James M. Cook[a,*]

[a]Department of Chemistry, University of Wisconsin—Milwaukee, Milwaukee, WI 53201, USA
[b]Department of Chemistry, University of Virginia, McCormick Road, Charlottesville, VA 22904, USA
[c]Antibiotics Laboratory, Discovery Research Institute, RIKEN, 2-1 Hirosawa, Wako-shi, Saitama 351-0198, Japan

Abstract—Tryprostatin A is an inhibitor of breast cancer resistance protein, consequently a series of structure–activity studies on the cell cycle inhibitory effects of tryprostatin A analogues as potential antitumor antimitotic agents have been carried out. These analogues were assayed for their growth inhibition properties and their ability to perturb the cell cycle in tsFT210 cells. SAR studies resulted in the identification of the essential structural features required for cytotoxic activity. The absolute configuration L-Tyr-L-pro in the diketopiperazine ring along with the presence of the 6-methoxy substituent on the indole moiety of 1 was shown to be essential for dual inhibition of topoisomerase II and tubulin polymerization. Biological evaluation also indicated the presence of the 2-isoprenyl moiety on the indole scaffold of 1 was essential for potent inhibition of cell proliferation. Substitution of the indole N_a–H in 1 with various alkyl or aryl groups, incorporation of various L-amino acids into the diketopiperazine ring in place of L-proline, and substitution of the 6-methoxy group in 1 with other functionality provided active analogues. The nature of the substituents present on the indole N_a–H or the indole C-2 position influenced the mechanism of action of these analogues. Analogues 68 ($IC_{50} = 10 \mu M$) and 67 ($IC_{50} = 19 \mu M$) were 7-fold and 3.5-fold more potent, respectively, than 1 ($IC_{50} = 68 \mu M$) in the inhibition of the growth of tsFT210 cells. Diastereomer-2 of tryprostatin B 8 was a potent inhibitor of the growth of three human carcinoma cell lines: H520 ($IC_{50} = 11.9 \mu M$), MCF-7 ($IC_{50} = 17.0 \mu M$) and PC-3 ($IC_{50} = 11.1 \mu M$) and was equipotent with etoposide, a clinically used anticancer agent. Isothiocyanate analogue 71 and 6-azido analogue 72 were as potent as 1 in the tsFT210 cell proliferation and may be useful tools in labeling BCRP.
© 2008 Elsevier Ltd. All rights reserved.

1. Introduction

The cell cycle coordinates a variety of cellular functions involved in the accurate replication of the genome and cell division.[1] These processes are tightly regulated primarily at the G_1/S and G_2/M phase transitions by a series of checkpoints. It has become clear that checkpoint control defects in cancer cells contribute to tumorigenesis and are a significant reason for the increased selectivity of tumors over normal cells towards chemotherapy.[2,3] Cell cycle inhibitors or modulators

are highly promising new therapeutic agents against human cancers.

With an increased understanding of the molecular biology of cell cycle control it has become possible to develop bioassays and screen for agents that specifically interfere with these processes. One such method was developed by Osada et al.[4,5] which utilizes the synchronous culture of the murine temperature-sensitive mutant cell line, tsFT210, defective in the $p34^{cdc2}$ gene. With this assay a family of 2-isoprenylated diketopiperazine indole alkaloids which effect cell cycle arrest at the G2/M phase was isolated from the fermentation broth of a marine fungal strain of *Aspergillus fumigatus* BM939. It was found that tryprostatin A 1 (Chart 1) and tryprostatin B 2 (Chart 1) completely inhibited cell cycle

1 R = OMe, tryprostatin A
2 R = H,   tryprostatin B

azatoxin

etoposide

vinblastine R = CH₃
vincristine R = CHO

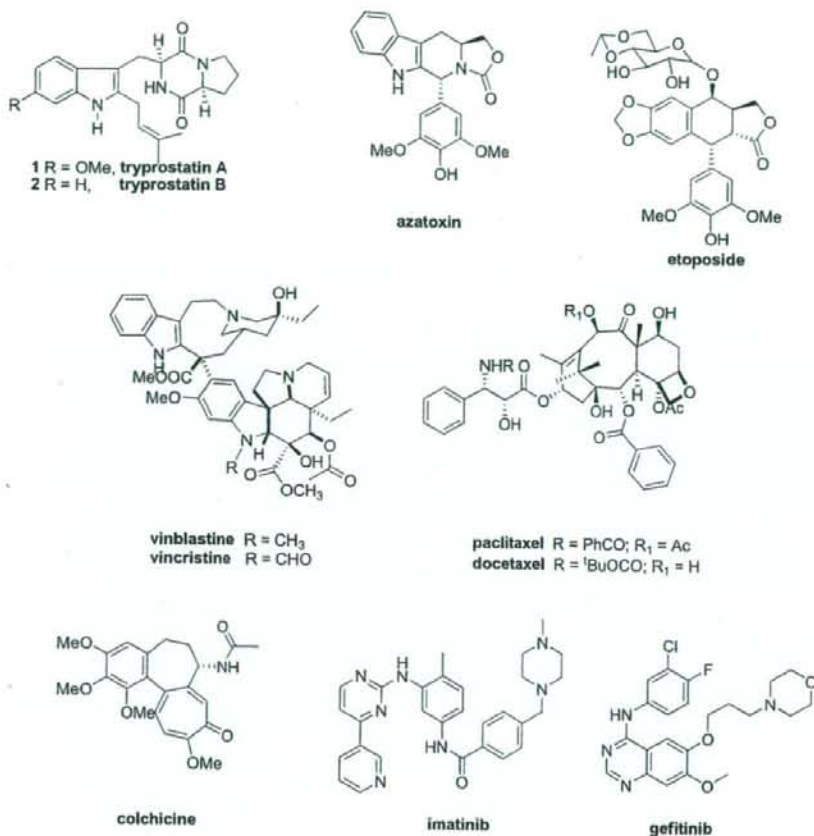paclitaxel R = PhCO; R₁ = Ac
docetaxel R = ᵗBuOCO; R₁ = H

colchicine

imatinib

gefitinib

Chart 1.

progression of tsFT210 cells in the G2/M phase at a final concentration of 50 μg/mL of **1** and 12.5 μg/mL of **2**, respectively.[6–8] Since these indole alkaloids were isolated only in small amounts, studies on the mechanism and SAR were not reported earlier.

Tryprostatin A and B have previously been synthesized,[9–11] the aim of which was to study their mechanism of action. The similarities in the structures of the tryprostatins with etoposide (Chart 1) and azatoxin (Chart 1), a dual inhibitor of topoisomerase II (G2)/tubulin polymerization (M), led to the investigation of the ability of the two tryprostatins to inhibit topoisomerase II and tubulin polymerization. Biological evaluations[12] of **1** and **2** indicated that both alkaloids were very weak inhibitors of topoisomerase II in the topoisomerase II assay; while only **1** had marginal activity in the tubulin polymerization assay. This latter result was in agreement with the data reported for **1** by Osada et al.[13] Osada et al.[13] also reported **1** inhibited cell cycle progression of rat normal fibroblast 3Y1 cells specifically in the M phase. The concentration of **1** that arrested cell cycle progression in the M phase corresponded to that which induced a marked depolymerization *in situ* of the microtubules containing both

cytoplasmic network and spindle apparatus. Although tryprostatin B **2** arrested cell cycle progression at a lower concentration than **1**, the inhibition was not due to inhibition of the M phase. It was shown that **1** inhibited microtubule assembly through a different type of mechanism than colchicine (Chart 1), vinblastine (Chart 1), or maytansine–rhizoxin.[13] Tryprostatin A **1** inhibited microtubule assembly by interfering with the interaction between microtubule-associated proteins (MAPs) and the C-terminal domain of tubulin. Since **1** operated by an entirely novel mechanism this may be important in cancer chemotherapy, especially in multiple drug resistance (MDR) cancers.

Microtubules are hollow cylindrical tubes found in almost all eukaryotic cell types. They play an important role in a variety of cellular functions, such as cell division, cell movement, cell shape, and transport of organelles inside the cell.[14] Tubulin exists as a heterodimer of α- and β-tubulin and is the major building block of microtubules. Proteins such as the MAPs bind to and modify microtubule properties.[14,15] In the absence of MAPs, α/β-tubulin heterodimers polymerize only by treatment with high concentrations of glycerol or organic acids such as glutamate.[16]

The discovery of numerous compounds from natural sources which display a wide structural diversity and are cytotoxic by perturbation of the dynamic instability of microtubules has attracted much attention within the last two decades.[17–20] Microtubules have, therefore, become an attractive pharmacological target for anticancer drug discovery.[17–20] Almost all antimitotic agents interact with the α/β-tubulin dimer, rather than microtubule-associated proteins (MAPs) or other proteins involved in microtubule functions. The *Vinca* alkaloids, exemplified by vinblastine (Chart 1) and vincristine (Chart 1), as well as the taxanes, such as paclitaxel (Chart 1) and the semisynthetic analogue docetaxel (Chart 1), are the most commonly used antimitotic agents in the clinical treatment of cancer.[21] Colchicine is another important antimitotic agent; however, it has limited medicinal utility due to its narrow therapeutic index.

Additionally, the natural products combretastatin A-4,[22] curacin A,[23] podophyllotoxin,[24] epothilones A and B,[25] and dolastatin[26] to cite just a few, are known to be cytotoxic through binding interactions with tubulin. Another antimitotic agent, estramustine phosphate inhibits microtubule assembly by binding to both microtubule-associated protein 2 (MAP2) and tubulin,[27] while 5,5'-bis[8-(phenylamino)-1-naphthalenesulphonate] (bis-ANS) specifically inhibits MAP-dependent microtubule assembly by interaction with the C-terminal domain of the tubulin heterodimer.[28] These compounds may lead to useful cancer therapeutic agents. Indeed, estramustine in combination with other antimicrotubule agents exhibits synergistic cytotoxicity both in vitro and in vivo.[27] However, no new tubulin polymerization inhibitor of low molecular weight has reached clinical status, as yet. Clinically available compounds such as paclitaxel or vincristine face several disadvantages; principally: (i) high toxicity, (ii) development of drug resistance in patients, (iii) marginal oral bioavailability and poor solubility, and (iv) complex synthesis or isolation proce-

dures.[17–20] Therefore, a pressing need to develop simpler, more effective antitumor drugs still remains.

The development of MDR to chemotherapeutic agents remains one of the primary obstacles in cancer treatment. These arise from intrinsic or acquired mechanisms of resistance. The overexpression of energy dependent (ATP) transmembrane drug-efflux pumps, such as P-glycoprotein (MDR1), multidrug resistance protein (MRP), and breast cancer resistance protein (BCRP), have been shown to produce resistance to several commonly used chemotherapeutic agents. Breast cancer resistance protein is a 72 kDa protein which probably homodimerizes to form an active transport complex.[29] BCRP was first identified in drug resistant MCF-7/adrVp cells[30] and has been recently reviewed.[31–33] Like other members of the ATP binding cassette family of membrane transporters, such as MDR1 and MRP1, BCRP is expressed in a variety of malignancies where it may produce resistance to chemotherapeutic agents. In addition, it has also been reported that BCRP expression may be a prognostic indicator in certain cancers and is associated with poor response to chemotherapy.[34,35] Overexpression of BCRP has been reported in a number of tumor types including: adenocarcinomas (arising from the digestive tract, the endometrium, and the lung), melanoma, soft tissue sarcomas,[36] hematological malignancies such as acute myeloid leukemia (AML),[37] and acute lymphoblastic leukemia (ALL).[38] Elevated expression of BCRP results in resistance of various cancer cell lines to antitumor drugs including: topotecan, mitoxantrone, daunorubicin, doxorubicin, and bisantrene.[39] In addition, flavopiridol resistance is mediated by BCRP.[40]

The clinical significance of BCRP along with its limited expression in normal tissues makes BCRP a viable target for inhibition to reverse MDR. Several potent and specific inhibitors of BCRP have been developed. This has potentially opened the door to clinical applications of BCRP inhibition. These inhibitors include the
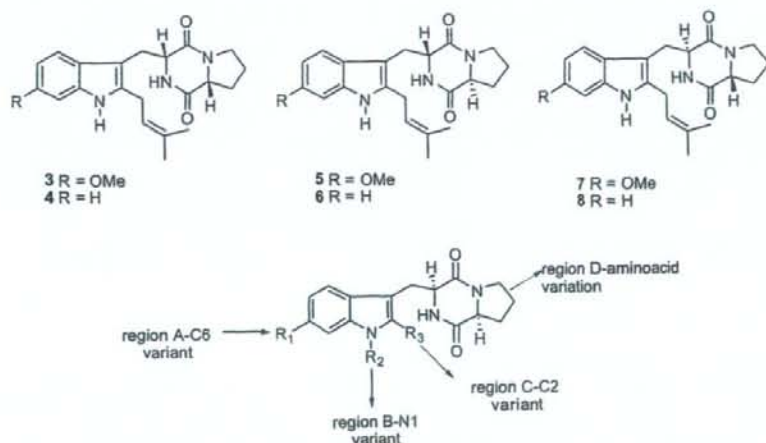

3 R = OMe
4 R = H

5 R = OMe
6 R = H

7 R = OMe
8 R = H

region A-C6 variant → R₁
region B-N1 variant → R₂
region C-C2 variant
region D-aminoacid variation
R₃

Figure 1.

targeted agents: gefitinib and imatinib mesylate,[41] as well as the more specific inhibitors: fumitremorgin C,[42] tryprostatin A,[43] and GF120918.[44] At concentrations of 10–50 μM, tryprostatin A **1** was shown to reverse a mitoxantrone-resistant phenotype and inhibited the cellular BCRP-dependent mitoxantrone accumulation in the human gastric carcinoma cell line EPG85-257RNOV and the human breast cancer cell line MCF-7/AdrVp (both exhibited acquired BCRP-mediated MDR). No cytotoxicity was observed at effective concentrations.[43]

In the search for potent and selective antitumor agents, the synthesis of a series of analogues (**3–8**, Fig. 1) of **1** and **2** was carried out in order to probe the importance of the stereochemistry of the diketopiperazine ring on the inhibition of topoisomerase II and/or tubulin polymerization. Tryprostatin analogues **1–8** were evaluated for their ability to inhibit topoisomerase II and/or tubulin binding protein as well as their tumor cell growth inhibitory activity.[12]

More recently, Osada et al.[13] reported the presence of the 6-methoxy substituent on the indole moiety of **1** conferred lower cytotoxicity to tryprostatin A and enhanced the specificity for inhibition of microtubule assembly.

The lower cytotoxicity of **1** in comparison to **2**, combined with a unique mechanism for inhibition of tubulin polymerization, as well as BCRP prompted investigation of the structure activity relationships (SAR) in **1** in order to enhance tubulin polymerization and/or BCRP inhibition. To our knowledge, no SAR of tryprostatin A has appeared in the literature, to date. The SAR studies were designed to determine the minimum structural requirements of tryprostatin A required to exhibit potent and selective cytotoxic activity, in the search for new anticancer agents. Several modifications, which maintained the same backbone, were carried out as outlined in Figure 1: (A) substitution of the 6-position of the aromatic ring, (B) alkylation of the indole NH, (C) substitution of the 2-position of the indole moiety, and (D) substitution of the L-proline residue in the diketopiperazine ring with other L-amino acids.

2. Chemistry

The synthesis of optically active **1** and **2** have been reported.[9–11] This method was also extended to the synthesis of the enantiomers (**3** and **4**) and diastereomers (**5–8**) of **1** and **2** (Scheme 1).[11,12] The synthesis of **1–8**
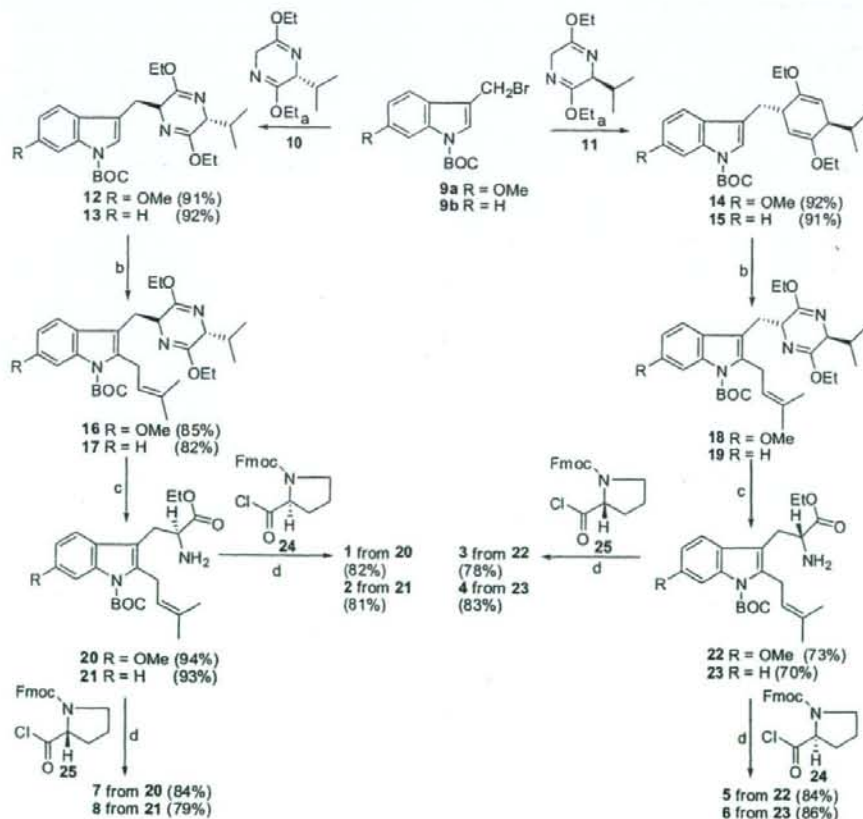
Scheme 1. Reagents and conditions: (a) THF, *n*-BuLi, −78 °C; (b) LDA (1.5 equiv), THF, isoprenylbromide (3 equiv); (c) 2 N aq HCl, THF, −78 °C to rt; (d) TEA, CHCl₃; DEA, CH₃CN, rt; xylene. reflux.

(Scheme 1) began with indoles **9a** and **9b** which were coupled with the anion of the Schöllkopf chiral auxiliary **11** (derived from L-valine), to afford the *trans* diastereomers **14** and **15**, respectively, with 100% diastereoselectivity. The diastereoselectivity of the addition to the Schöllkopf chiral auxillary was found to be 100% by analysis of the ^{1}H spectrum of the crude mixture of the respective compounds. When indoles **14** and **15** were treated with LDA at −78 °C, followed by addition of isoprenyl bromide, the 2-isoprenylpyrazine derivatives **18** and **19** were obtained, respectively. The pyrazine moiety was removed from pyrazines **18** or **19** under acidic conditions (aq HCl, THF) in 94% yield to afford the 2-isoprenyl tryptophan **22** or **23**, respectively. The coupling of 2-isoprenyl tryptophan **22** or **23** with Fmoc-D-proline **25** using triethylamine as the base was followed by formation of the diketopiperazine ring. The Boc protecting group was removed from the indole N(H) function in refluxing xylene to afford **3** and **4**, respectively. Similarly, coupling of 2-isoprenyl tryptophan **22** or **23** with Fmoc-L-proline **24** afforded **5** or **6**, respectively. The natural products (**1** and **2**) were prepared from the *trans* transfer of chirality from D-valine (Schöllkopf) and from L-proline.[9–11] The diastereomers **7** and **8** of **1** and **2**, respectively, were prepared from the *trans* transfer of chirality from D-valine (Schöllkopf) and from D-proline, as outlined in Scheme 1.[9–11]

Analogues **37–40** were intended as tryprostatin A mimics in which the alkyl substituent was moved from the indole 2-position to the indole NH. This was expected to result in analogues that are more readily accessible than the natural products which require methods for prenylation of tryptophan at C-2. As shown in Scheme 2, the *ortho*-iodoaniline **26** was coupled with the internal alkyne[10] **27** in the presence of catalytic Pd(OAc)$_2$ with Na$_2$CO$_3$ as the base to provide indole **28** in 77% yield.[45,46]

Alkylation of **28** with methyl iodide, isoprenyl bromide, benzyl bromide or allyl bromide in the presence of so-

dium hydride afforded the indole N$_a$-substituted analogues **29–32** in 72–99% yields. Hydrolysis of pyrazines **29–32** with 2 N aq HCl in THF resulted in removal of both the bislactim ether moiety and the silyl group. Tryptophans **33–36** were readily transformed into analogues **37–40** of tryprostatin A under conditions analogous to the steps in Scheme 1.

In order to synthesize the N$_a$-substituted analogues (**46** and **47**) of **1**, in region B in which the indole 2-position carried the isoprenyl group, an analogous strategy was employed. Thermal removal of the Boc protecting group of **16** (Scheme 3) in refluxing xylene afforded pyrazine **41**. Alkylation of **41** with benzyl bromide or allyl bromide using sodium hydride afforded analogues **42** and **43** in 91% and 82% yields, respectively. These intermediates were readily transformed into analogues **46** and **47** of tryprostatin A under conditions analogous to the steps in Scheme 1, as illustrated in Scheme 3.
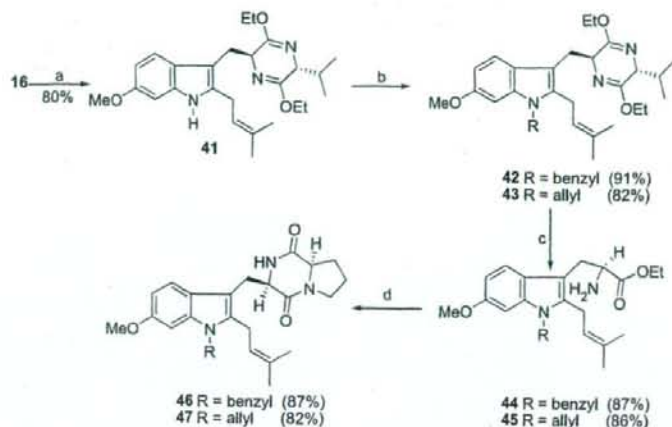
To obtain analogues with different substitution at the indole 2-position (region C) of **1**, 2-bromo-indole **48** (Scheme 4) served as a common intermediate which was easily obtained from indole **28** after sequential treatment with NBS and Boc anhydride. As shown in Scheme 4, lithium–halogen exchange, followed by treatment with benzyl bromide or allyl bromide furnished the 2-substituted analogues **49** and **50**. Analogues **49** and **50** were further transformed into 2-substituted indoles **55** and **56**, respectively, under standard conditions (Scheme 4). For the synthesis of **51** (Scheme 4), the zinc reagent was prepared through lithium–halogen exchange followed by treatment with zinc chloride. Negishi coupling[47] of the zinc reagent with phenyl iodide using Pd(OAc)$_2$ in the presence of trifuryl phosphine afforded the 2-phenyl indole **51** in 65% yield which was then transformed to analogue **57** under conditions outlined in Scheme 4. A variety of other conditions were attempted to prepare the 2-phenyl indole **51**, however the Negishi coupling was the only method that was successful in a practical sense.
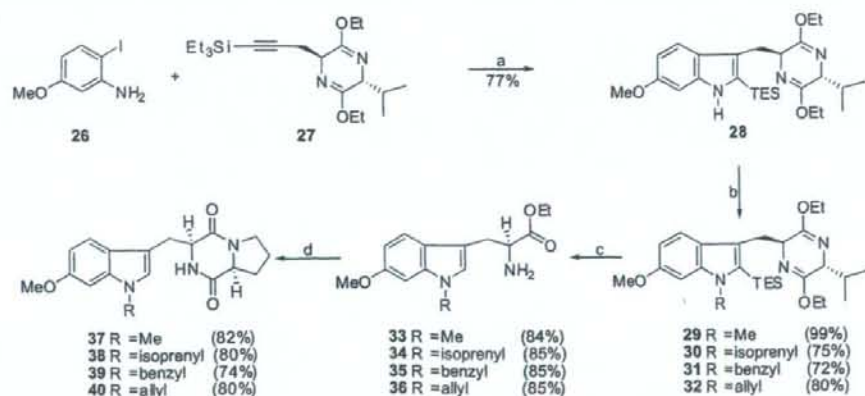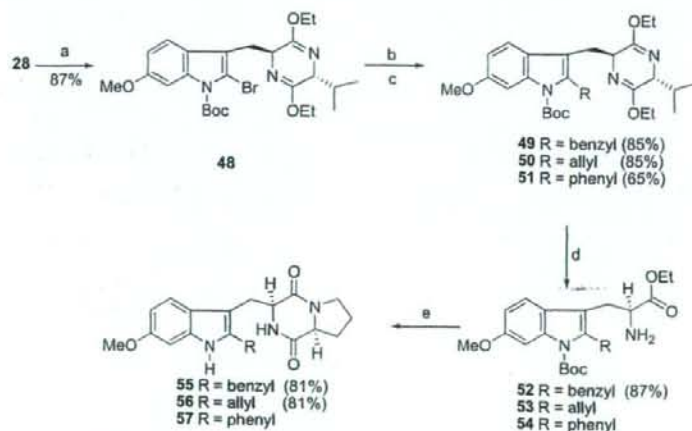

Scheme 2. Reagents and conditions: (a) Pd(OAc)$_2$, LiCl, Na$_2$CO$_3$, DMF, 100 °C, 77%; (b) NaH, DMF, RX; (c) 2 N aq HCl, EtOH, THF, −78 °C to rt; (d) 24, TEA, CHCl$_3$; DEA, CH$_3$CN, rt; xylene, reflux.

Heck coupling[48] of bromide **48** with methyl acrylate in the presence of 5% Pd(PPh₃)₄ and Cy₂NEt afforded the coupled product **58** in 94% yield (Scheme 5). Analogue **58** (Scheme 5) was then transformed into ester

42 R = benzyl (91%)
43 R = allyl (82%)

46 R = benzyl (87%)
47 R = allyl (82%)

44 R = benzyl (87%)
45 R = allyl (86%)

Scheme 3. Reagents and conditions: (a) xylene, reflux, 80%; (b) NaH, DMF, RX; (c) 2 N aq HCl, EtOH, THF, −78 °C to rt; (d) **24**, TEA, CHCl₃; DEA, CH₃CN, rt; xylene, reflux.

48

49 R = benzyl (85%)
50 R = allyl (85%)
51 R = phenyl (65%)

55 R = benzyl (81%)
56 R = allyl (81%)
57 R = phenyl

52 R = benzyl (87%)
53 R = allyl
54 R = phenyl

Scheme 4. Reagents and conditions: (a) NBS, CH₃CN; (Boc)₂O, DMAP, CH₃CN, rt, 87%; (b) n-BuLi, THF, −78 °C; RX; (c) n-BuLi, THF, −78 °C; ZnCl₂; Pd(OAc)₂, PhI, tri-2-furyl phosphine, rt, 65%; (d) 2 N aq HCl, EtOH, THF, −78 °C to rt; (e) **24**, TEA, CHCl₃; DEA, CH₃CN, rt; xylene, reflux.

48

58

60

59
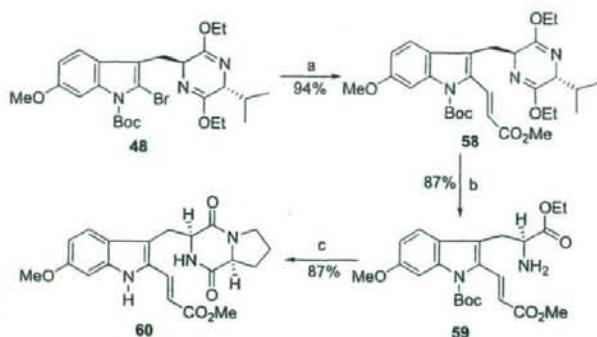
Scheme 5. Reagents and conditions: (a) Pd(PPh₃)₄, methyl acrylate, Cy₂NMe, toluene, 95 °C, 94%; (b) 2 N aq HCl, EtOH, THF, −78 °C to rt, 80%; (c) **24**, TEA, CHCl₃; DEA, CH₃CN, rt; xylene, reflux.
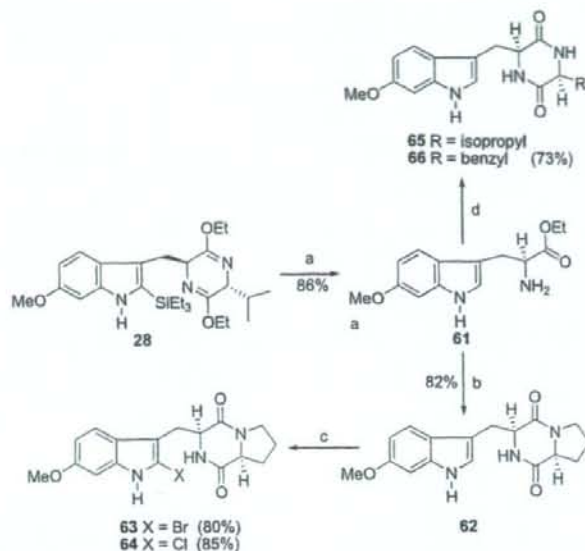
Scheme 6. Reagents and conditions: (a) 2 N aq HCl, EtOH, THF, −78 °C to rt, 86%; (b) **24**, TEA, CHCl₃, DEA, CH₃CN, rt; xylene, reflux; (c) NBS or NCS, THF, −78 °C to rt; (d) Fmoc-ʟ-amino-acyl chloride, TEA, CHCl₃; DEA, CH₃CN, rt; xylene, reflux.

60, analogous to well-developed processes outlined previously in Scheme 1. It was well known in the literature that the 6-methoxy group activated the C-2 position of the indole nucleus towards electrophilic substitution. As illustrated in Scheme 6, indole **28** was hydrolyzed with aq 2 N HCl to afford the 6-methoxy-ʟ-tryptophan ethyl ester **61** in 86% yield. Ester **61** was further transformed into the N$_a$–H analogue **62** under conditions similar to that described for **1** in Scheme 1. Analogue **62** was treated with NBS at −78 °C to afford 2-bromo-indole **63** in 80% yield. The corresponding 2-chloro analogue **64** was prepared in 85% yield (from NCS) under analogous conditions to those described above for the preparation of 2-bromo-indole **63**.
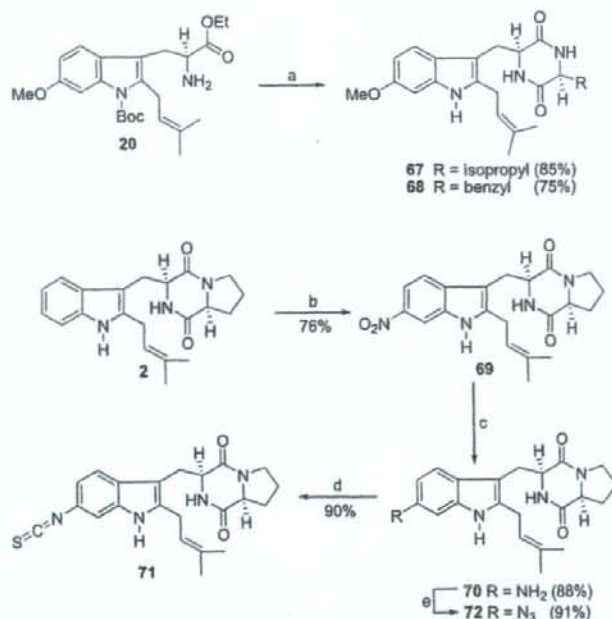
Scheme 7. Reagents and conditions: (a) Fmoc-ʟ-amino-acylchloride, TEA, CHCl₃; DEA, CH₃CN, rt; xylene, reflux; (b) NaNO₂, TFA, −78 °C to −20 °C, 75%; (c) NH₂NH₂, FeCl₃.6H₂O, active C, MeOH, reflux, 91%; (d) CHCl₃, ClC(S)Cl, 93%; (e) TfN₃, aq CuSO₄, Et₃N, CH₂Cl₂/MeOH, 89%.

Two additional amino acids, other than proline, were also incorporated into 1 (region D). As shown in Scheme 6, 6-methoxytryptophan 61 was transformed into the cyclic dipeptides 65 and 66 with L-valine and L-phenylalanine, respectively, under conditions illustrated in Scheme 6. The 2-isoprenyl indole 20 was also transformed to analogues 67 and 68, as shown in Scheme 7.

The synthesis of C-6 substituted analogues of tryprostatin A modified in region A is depicted in Scheme 7. The synthesis began with a highly regioselective process for nitration of 2. Although several methods were attempted to incorporate the nitro group at the desired 6-position with only minimal success, this was successfully carried out when 2 was treated with $NaNO_2$ in the presence of TFA[49] at low temperature to afford 69. To determine the regiochemistry, detailed NMR analysis of the 6-nitro analogue 69 was carried out. The coupling patterns of the aromatic ring protons could be employed to distinguish the 4- and 7-substituted indoles from the 5- and 6-substituted regioisomers, since one would not expect singlet protons in the spectrum of the 4- or 7-substituted indoles. The ^1H NMR spectrum of 69 clearly contained one singlet (8.29 ppm) corresponding to one proton in the aromatic region, consequently, the product of this mononitration was either the 5- or 6-substituted regioisomer. In case of the 5-nitrosubstituted indole this singlet would correspond to the proton at C(4), whereas in the case of 6-nitrosubstituted indole this singlet would correspond to the proton at C(7). The 6-nitro regioisomer would be expected to exhibit a much stronger NOE signal between the indole N(H) proton and the proton at C(7) than the one between the indole N(H) proton and the proton at C(4). A strong NOE signal was observed between this proton singlet and the indole N(H) and vice versa. This further ruled out the 5-nitro regioisomer. Reduction of the nitro group in 69 (Scheme 7) with hydrazine in the presence of $FeCl_3.H_2O$ and activated carbon in refluxing methanol[45] furnished analogue 70 which was purified by column chromatography and stored as the hydrochloride salt. Amine 70 was stirred with thiophosgene in dry chloroform to afford the 6-isothiocyanate analogue 71 in high yield. Treatment of amine 70 with triflyl azide (TfN_3) in the presence of copper sulfate afforded analogue 72 in 89% yield.[50,51]

3. Biological evaluation and discussion

3.1. Effects of analogues 1–8 on topoisomerase II

Tryprostatins 1–8 were evaluated as inhibitors of topoisomerase II in the topoisomerase II-mediated DNA relaxation assay.[52,53] This assay measures the ability of the compound to inhibit the ability of topoisomerase II to relax supercoiled DNA. The inhibitory activities against topoisomerase II of compounds 1–8 were evaluated by agarose gel electrophoresis experiments. The photopicture of 1–4's agarose gel electro-
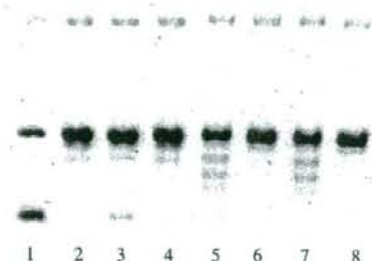

Figure 2. Representative agarose gel from the topoisomerase II-mediated DNA relaxation assay. Data for all compounds are not shown. Lane 1: DNA only; lane 2: DNA + topoisomerase II; lane 3: DNA + topoisomerase II + m-AMSA (100 μM); lane 4: DNA + topoisomerase II + 1% DMSO; lane 5: DNA + topoisomerase II + 1 (100 μM); lane 6: DNA + topoisomerase II + 3 (100 μM); lane 7: DNA + topoisomerase II + 2 (100 μM); lane 8: DNA + topoisomerase II + 4 (100 μM).

phoresis experiment is presented in Figure 2. The agent, m-AMSA, a known inhibitor of topoisomerase II, was employed as the control (lane 3). The other controls employed were no-enzyme (lane 1), enzyme (lane 2), and 1% DMSO (lane 4). The gels were analyzed qualitatively by examination of the presence of DNA bands that migrate farther down on the gel than the negative controls. Topoisomerase II-mediated relaxation of the DNA prevents the band from migrating down the gel as far as one that is still in a supercoiled form. Therefore, DNA incubated with topoisomerse II inhibitors will migrate farther on the gel than the no-enzyme or DMSO controls. Lane 1 is DNA alone, existing in two forms- supercoiled DNA and loosened DNA; lane 2 is topoisomerase II together with DNA, and supercoiled DNA was relaxed by topoisomerase II completely. As illustrated in Figure 2, 1 (lane 5) and 2 (lane 7) are both weak inhibitors of topoisomerase II; however, the potency cannot be determined from this data. The laddering is evidence of inhibition of topoisomerase II. The enantiomers of tryprostatin A 3 (lane 6) and B 4 (lane 8) were both inactive. The four diastereomers 5–8 (data not shown) were also found to be inactive as topoisomerase II inhibitors in this assay. Tryprostatin A 1 and B 2 are, therefore, weak inhibitors of topoisomerase II but their enantiomers (3 and 4) and diastereomers (5–8) are not.

3.2. Effects of analogues 1–8 on tubulin polymerization

Tryprostatins 1–8 were also evaluated as inhibitors of tubulin polymerization.[13,54] Purified tubulin, containing MAPs and GTP, was incubated at 37 °C with either DMSO (as a solvent control), colchicine (standard), or analogues 1–8 and the change in absorbance was measured at 351 nM over 10 min. The concentration of the standard (colchicine) and analogues (1–8) was varied for different runs to obtain a delta absorbance versus concentration curve. Illustrated in Figures 3 and 4 are the results of the tubulin polymerization assay. Colchicine (the positive control) strongly suppressed tubulin
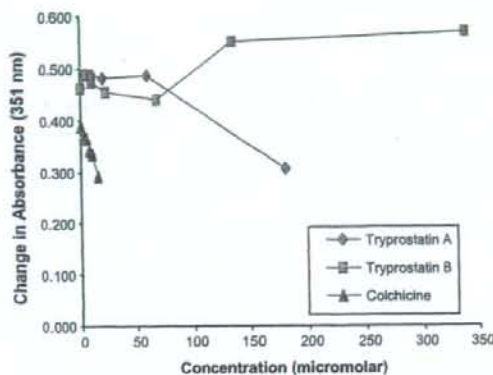
Figure 3. Inhibition of tubulin polymerization by tryprostatin A **1** and B **2**, colchicine, a known tubulin polymerization inhibitor, was used as a control.
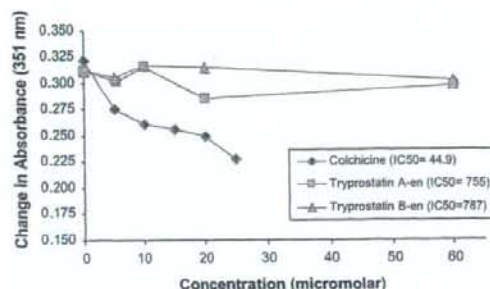

Figure 4. Inhibition of tubulin polymerization by analogues **3** and **4**. Colchicine was employed as a control.

assembly (IC_{50} = 44.9 μM), while **1** (Fig. 3) caused a moderate reduction in the rate of tubulin polymerization (IC_{50} = 250 μM). Tryprostatin B **2** (Fig. 3) as well as the enantiomers of tryprostatin A **3** and B **4** (Fig. 4) were inactive in this assay (IC_{50s} > 700 μM). Compounds **5–8** (data not shown) were also found to be inactive in this assay (less than 2% inhibition at 60 μM: IC_{50s} > 700 μM).

Osada et al.[13] recently reported that tryprostatin A **1** was a novel inhibitor of MAP-dependent microtubule assembly and through disruption of the microtubule spindle, specifically inhibited cell cycle progression at the M phase. Thus biological evaluation of analogues **1–8** illustrated above indicated that **1** was a weak inhibitor of both topoisomerase II and tubulin polymerization, whereas **2** was only a weak inhibitor of topoisomerase II. The enantiomers (**3** and **4**) and diastereomers (**5–8**) were inactive in both the tubulin polymerization assay and topoisomerase II-mediated DNA relaxation assay. In terms of the stereochemistry of the amino acids present in the diketopiperazine ring, biological evaluation indicated that ligands with the absolute configuration L-Tyr-L-Pro (natural stereochemistry as in **1** and **2**) were essential for inhibition of tubulin polymerization and/or topoisomerase II. Modification of the absolute configuration of the diketopiperazine ring from L-Tyr-L-Pro (**1** and **2**) to D-Tyr-D-Pro (**3** and **4**), D-Tyr-L-Pro (**5** and **6**), and L-Tyr-D-Pro (**7** and **8**) resulted in analogues that were very poor inhibitors of topoisomerase II and/or tubulin polymerization. Additionally, comparisons of analogues **1** and **2** indicated that presence of the 6-methoxy substituent in **1** resulted in analogues that are dual inhibitors of microtubule assembly and topoisomerase II.

In order to determine whether the absolute configuration of L-Tyr and/or L-Pro in the diketopiperazine ring was required to inhibit cell proliferation, analogues **1–8** were evaluated as inhibitors of three human lung (H520), breast (MCF-7), and prostrate (PC-3) cancer cell lines (Table 1).[12] Analogues **1–7** were not potent inhibitors (GI_{50} > 100 μM) of the growth of tumor cells in the three human cancer cell lines evaluated. However, the diastereomer **8** of tryprostatin B **2** exhibited potent cytotoxic activity at 100 μM against all three human cancer cell lines evaluated. It was found, in agreement with Danishefsky et al.,[55] that the inhibition of tryprostatin B **2** against the growth of the three human cancer cell lines evaluated occurred at higher concentrations (GI_{50} > 100 μM) than that reported earlier[6–8] for isolated tryprostatin B **2**. Danishefsky et al.[55] have shed some light on the apparent discrepancies in the cytotoxicity of isolated **2** versus synthetic **2**. Their studies[55]

Table 1. Cell growth inhibition of tryprostatins **1–8** (at 10, 100 μM) on human lung (H520), breast (MCF-7) and prostate (PC-3) cancer cell lines[a]

Compound	Percent cell survival[b]					
	H520		MCF-7		PC-3	
	10 μM	100 μM	10 μM	100 μM	10 μM	100 μM
1	80.1 ± 4.1	79.4 ± 4.2	>100	95.0 ± 4.7	99.2 ± 4.2	95.6 ± 5.0
2	77.6 ± 3.6	60.5 ± 3.5	88.2 ± 5.8	66.7 ± 5.3	95.5 ± 2.8	68.9 ± 6.6
3	81.7 ± 3.9	75.2 ± 3.5	>100	>100	>100	83.7 ± 4.2
4	>100	99.8 ± 1.6	>100	>100	95.8 ± 1.3	78.9 ± 2.1
5	>100	>100	>100	>100	>100	>100
6	>100	76.5 ± 11.2	>100	>100	97.3 ± 5.9	68.5 ± 3.4
7	99.3 ± 1.8	98.5 ± 3.1	>100	99.0 ± 4.6	>100	>100
8	88.3 ± 8.4	0.1 ± 0.1	73.6 ± 5.3	0.0 ± 0.0	59.3 ± 3.9	0.2 ± 0.0

[a] Table 1 published in its entirety in Ref. 12.

[b] CellTiter 96™ AQ_ueous non-radioactive cell proliferation assay (Promega) was used to determine growth inhibition. Percent inhibition values were calculated versus control wells and were done in quadruplicate. Control wells contained 0.2% DMSO and the positive control was either etoposide or m-AMSA (20 μM, 20 μM). Values are reported ± the standard deviation of the mean.

Table 2. Growth inhibition (GI_{50}) in µM of human cancer cell lines by 8 and etoposide

Compound	H520	MCF-7	PC-3
8[a]	15.8	15.9	11.9
8	11.9	17.0	12.3
Etoposide	8.7	55.6	11.1

[a] Data were obtained from NCI.

indicated that a DMSO solution of **2**, upon standing in air, undergoes slow transformation to a mixture of products. The solutions of **2** containing detectable byproducts were considerably more cytotoxic (ca. 50-fold) than those containing apparently homogenous tryprostatin. Growth inhibitory (GI_{50}) potency of **8** was also compared to that of etoposide against the growth of the three human lung (H520), breast (MCF-7), and prostate (PC-3) cancer cell lines (Table 2).[12] Outlined in Table 2 are the results obtained from the National Cancer Institute (NCI)[56] screening of analogue **8** on the same three human cancer cell lines. The data obtained from the NCI for **8** were in complete agreement with the data obtained for **8** in the present study against all three human cancer cell lines evaluated. Analogue **8** was 3-fold more potent than etoposide in inhibition of the growth of the MCF-7 human cancer cell line. Also, analogue **8** was equipotent with etoposide against the growth of H520 and PC-3 human cancer cell lines.

If one examines the structures of tryprostatins (**1–7**) and compares them with that of the active analogue **8**, one can generate the following conclusion: the L-Tyr unit in the diketopiperazine ring was essential for potent tumor cell growth inhibition since none of the other tryprostatins (**3–6**), which contained the D-Tyr unit, exhibited activity. Biological evaluation of analogue **8** also indicated that the inhibition of the growth of human cancer cells by analogue **8** was not due to the inhibition of topoisomerase II or tubulin polymerization since analogue **8** was inactive against these two molecular targets. Further studies to identify the precise molecular targets are required. The presence of the 6-methoxy group on **7** compared to **8** nearly eliminated the potent tumor cell growth inhibitory activity against the three human cancer cell lines evaluated. The potent cytotoxic activity of analogue **8** against human cancer cells led to the evaluation of its activity against the growth of normal human cell lines. In preliminary studies, **8** was found to be cytotoxic to normal human cell lines; however, further studies are required in this regard.

Analogues **1–8** were selected by the NCI for evaluation in its in vitro preclinical antitumor screening program. The ability of compounds **1–8** to inhibit the growth of tumor cells was measured as GI_{50} values, the concentration required to inhibit the growth of tumor cells in culture by 50%, as compared to a control (Table 3). In two of the 60 tumor cell lines evaluated, tryprostatin A **1** showed GI_{50} values of $\leq 10^{-5}$ M. Again, tryprostatin B

Table 3. Cytotoxicity evaluation (GI_{50}, µM) of compounds **1–8** against selected tumor cell lines[56]

Cell line	1	2	3	4	5	6	7	8
Leukemia								
CCRF-CEM	>100	>100	>25	25.1	11.9	22.2	99.4	3.22
HL-60 (TB)	11.3	>100	>25	29.0	35.0	55.7	≥100	22.4
K-562	2.73	56.1	>25	25.8	17.7	31.8	>100	20.1
MOLT-4	ND	>100	>25	21.0	12.2	34.9	>100	5.96
RPMI-8226	37.1	>100	>25	12.9	7.76	18.6	92.0	5.54
SR	5.68	50.6	>25	12.1	11.3	25.4	76.9	9.46
Non-small cell lung cancer								
HOP-92	21.2	43.1	23.1	ND	ND	2.94	16.8	1.70
EKVX	>100	>100	>25	39.4	>50	20.7	>100	6.90
Colon cancer								
COLO 205	>100	>100	>25	21.2	12.4	39.3	>100	17.7
HT-29	ND	ND	ND	37.5	16.1	ND	40.3	5.25
Melanoma								
LOX IMVI	>100	>100	>25	>50	33.5	17.8	>100	9.23
Ovarian								
OVCAR-3	>100	>100	>25	38.2	>50	28.7	85.5	9.69
IGROV1	90.5	>100	>25	16.0	>50	32.3	50.0	11.5
Prostrate cancer								
PC-3	94.0	>100	>25	21.2	21.7	24.8	>100	11.9
DU-145	>100	>100	>25	>50	40.0	59.5	>100	14.0
Breast cancer								
MDA-MB-231/ATCC	>100	>100	>25	11.9	13.0	49.6	>100	14.9
BT-549	79.7	58.2	>25	7.21	9.77	26.9	>100	13.2
MCF-7	>100	>100	>25	40.0	25.5	25.9	>100	15.9
Renal cancer								
UO-31	>100	>100	>25	12.6	27.3	45.7	>100	14.7

2 (GI$_{50}$ > 40 µM) was considerably less active against the growth of the 60 tumor cell lines evaluated. In 9 of the 60 tumor cell lines evaluated, the most active analogue **8** showed GI$_{50}$ values of ≤10^{-5} M. Analogue **5**, the diastereomer of tryprostatin A, **1** was more active than **1** in the inhibition of the growth of tumor cells in most of the tumor cell lines evaluated. Analogues **3** and **7** were both considerably less active than **1** in inhibition of the growth of the tumor cells in the NCI screening program. However, analogue **4**, the enantiomer of tryprostatin B **2**, as well as both of the diastereomers **6** and **8** were more active than **2** in inhibition of the growth of tumor cells in most of the tumor cell lines evaluated. It is noteworthy that compounds **4**, **5**, **6** and **8** were not general cell toxins but showed selectivity both within a type of tumor cell line and across different tumor cell lines, with inhibitory values, which in some instances, differed by 100-fold.

3.3. Structure–activity relationships of tryprostatin A analogues

Because **1** was an inhibitor of BCRP, the tryprostatin A-related analogues (**37–40**, **46**, **47**, **55**, **56**, **60**, and **62–72**) were evaluated in vitro for the ability to disrupt the cell cycle and to inhibit tsFT210 cell proliferation.[4,13,58] The inhibitory potency (IC$_{50}$) values are listed in Table 4 and compared with tryprostatin A **1**.

A 30 µM concentration of **1** arrested cell cycle progression in the M phase, as previously reported.[8,13] Many of these analogues were found to have similar activity as tryprostatin A against tsFT210 cell proliferation. Analogue **38**, which closely resembled tryprostatin A, was inactive. Substitution of the 2-isoprenyl moiety in **38** with a smaller methyl substituent (**37**) also resulted in an inactive analogue. Replacement of the N_a-isoprenyl group in analogue **38** with an allyl group (**40**) resulted in an analogue that was equipotent to **1** in the inhibition of cell proliferation. Similarly, replacement of the N_a-isoprenyl group in **38** with a N_a-benzyl group **39** also resulted in an analogue that was equipotent to **1** in inhibiting cell proliferation. However, analogues **39** and **40** inhibited cell cycle progression at the G1 phase. The biological data of analogues **39** and **40** indicated substitution of the indole N(H) with a benzyl moiety or allyl moiety was highly conducive for inhibition of cell proliferation and caused cell cycle arrest in the G1 phase. Tryprostatin A **1** analogues in which the indole NH was substituted with a benzyl moiety **46** or allyl moiety **47** also afforded active analogues that were equipotent with **1** in inhibition of the growth of tsFT210 cells. However, this inhibition was not cell cycle dependent. Removal of the 2-isoprenyl group in **1** afforded analogue **62** which was inactive. Similarly, removal of the 2-isoprenyl group in **1** and substitution of it with a bromine atom **63** or chlorine atom **64** also resulted in

Table 4. Effect of tryprostatin A-related analogues on cell cycle progression and tsFT210 cell proliferation

Compound	R^1	R^2	R^3	R^4	R^5	IC$_{50}$ (µM)[a]	Effect on cell cycle arrest[b]
1	OMe	H	Isoprenyl	–(CH$_2$)$_3$–		68	M phase at 30 µM
37	OMe	Me	H	–(CH$_2$)$_3$–		>100	No effect[c]
38	OMe	Isoprenyl	H	–(CH$_2$)$_3$–		>100	No effect
39	OMe	Benzyl	H	–(CH$_2$)$_3$–		46	G1 phase at 100 µM
40	OMe	Allyl	H	–(CH$_2$)$_3$–		62	G1 phase at 100 µM
46	OMe	Benzyl	Isoprenyl	–(CH$_2$)$_3$–		55	No effect
47	OMe	Allyl	Isoprenyl	–(CH$_2$)$_3$–		75	No effect
55	OMe	H	Benzyl	–(CH$_2$)$_3$–		>100	No effect
56	OMe	H	Allyl	–(CH$_2$)$_3$–		60	G1, G2/M phase at 100 µM
60	OMe	H	H	–(CH$_2$)$_3$–		>100	No effect
62	OMe	H	H	–(CH$_2$)$_3$–		>100	No effect
63	OMe	H	Br	–(CH$_2$)$_3$–		96	No effect
64	OMe	H	Cl	–(CH$_2$)$_3$–		>100	No effect
65	OMe	H	H	Isopropyl	H	>100	No effect
66	OMe	H	H	Benzyl	H	100	M phase at 100 µM
67	OMe	H	Isoprenyl	Isopropyl	H	19	G1, G2/M phase at 100 µM
68	OMe	H	Isoprenyl	Benzyl	H	10	No effect
69	NO$_2$	H	Isoprenyl	–(CH$_2$)$_3$–		>100	No effect
70	NH$_2$	H	Isoprenyl	–(CH$_2$)$_3$–		>100	No effect
71	NCS	H	Isoprenyl	–(CH$_2$)$_3$–		50	G1, G2/M phase at 100 µM
72	N$_3$	H	Isoprenyl	–(CH$_2$)$_3$–		60	G1, G2/M phase at 100 µM

[a] Exponentially growing tsFT210 cells were treated with test compounds at 32 °C for 48 h. Cell viability was measured using the color reagent, WST-8^{TM}.

[b] Exponentially growing tsFT210 cells were treated with test compounds at 32 °C for 18 h. Then, flow cytometric analysis and nuclei staining were carried out, as described in Section 5.

[c] No effect even at 100 µM.

inactive analogues. Comparison of the analogues 62–64 with the activity of the active analogue 1 indicated the lipophilic 2-isoprenyl group in 1 played an important role in the inhibition of cell proliferation. The lipophilic 2-isoprenyl moiety may play an important role in the interaction with the molecular target and/or may increase the lipophilicity of the molecule thereby facilitating passive diffusion into the cells. Substitution of the 2-isoprenyl group of 1 with a 2-benzyl group 55 or 2-methyl acrylate moiety 60 afforded inactive analogues. However, a 2-allyl substituted analogue 56 of 1 was found to be equipotent to 1 in the inhibition of cell proliferation. Analogue 56 also arrested cell cycle progression at the G1, G2/M phase. Substitution of the L-proline residue in the diketopiperazine ring of 1 with an L-valine residue (67) afforded a 3.5-fold more potent inhibitor of the growth of tsFT210 cells than 1. Similarly replacement of the L-proline residue in 1 with an L-phenyl alanine residue (68) resulted in an analogue that was 7-fold more potent than 1 in the inhibition of the growth of tsFT210 cells, but this inhibition was not cell cycle dependent. The biological data of analogues 67 and 68 indicated substitution of the L-proline residue in the diketopiperazine ring of 1 with other L-amino acids was highly conducive for inhibition of cell proliferation. Removal of the 2-isoprenyl group from analogue 67 afforded 65 which slightly inhibited ($IC_{50} > 100 \mu M$) cell proliferation. Again, removal of the 2-isoprenyl moiety from analogue 68 afforded analogue 66 which was 10-fold less potent than 68 in the cell proliferation assay again indicating the importance of the 2-isoprenyl moiety in the inhibition of cell proliferation. Analogue 66 also arrested cell cycle progression in the M phase at 100 μM. Replacement of the 6-methoxy group in 1 with a nitro group (69) or amino group (70) resulted in analogues that were poor ($IC_{50} > 100 \mu M$) inhibitors of the growth of tsFT210 cells. However, substitution of the 6-methoxy group in 1 with an isothiocyanate group 71 or azide group 72 resulted in analogues that were equipotent with 1 in the inhibition of the growth of tsFT210 cells. Both compounds 71 and 72 inhibited the cell cycle progression of tsFT210 cells at the G1, G2/M phase.

Turner and Sullivan et al.[57] have recently shown that tryprostatin A 1 is a specific and potent inhibitor of BCRP (breast cancer resistance protein), which further indicates the potential of analogues of tryprostatin A 1 synthesized in the present study in the potential inhibition of BCRP. Some of the analogues are currently being evaluated as inhibitors of BCRP and will be a topic of future communication. The isothiocyanate analogue 71 and the 6-azido analogue 72 may be excellent irreversible inhibitors in studies of BCRP.

4. Conclusion

In summary, the first structure–activity investigation into the cell cycle inhibitory effects of the tryprostatin A 1 analogues has been carried out. The SAR of tryprostatin A 1 suggests that the search for a potent and selective antitumor agent, in the tryprostatin series, still looks promising. Studies on elucidation of the mecha-

nism of action of the tryprostatins indicate that tryprostatin A 1 is a weak inhibitor of topoisomerase II and tubulin polymerization, whereas tryprostatin B 2 is only a weak inhibitor of topoisomerase II. The absolute configuration of L-Tyr-L-pro in the diketopiperazine ring of the tryprostatins was shown to be essential for inhibition of tubulin polymerization and/or topoisomerase II. The 6-methoxy substituent in 1 was shown to promote inhibition of both topoisomerase II and tubulin polymerization in in vitro assays. Biological evaluation indicated that the presence of the 2-isoprenyl moiety on the indole scaffold in 1 was essential for inhibition of cell proliferation. Removal of the 2-isoprenyl group in 1 and substitution of the indole NH with a benzyl group or allyl group also afforded analogues that inhibited cell proliferation. The 6-methoxy substituent in 1 could be replaced with various groups to afford active analogues. Various L-amino acids other than L-proline could be incorporated into the diketopiperazine ring of 1 to afford active analogues. The nature of the substituent present on the indole NH or at the C-2 position influenced the mechanism of action of the analogue and highlights the versatility of the tryprostatin skeleton as a template for drug discovery. Analogue 8 was more potent than etoposide (a clinically used anticancer drug) against the three human cancer cell lines evaluated. However, preliminary biological evaluation against normal cells indicated that it was toxic which may limit its potential use in this regard. More work is required to define this. In the NCI preclinical screening program analogue 5, the diastereomer of tryprostatin A 1, was more active than 1 in the inhibition of growth of tumor cells in most of the tumor cell lines evaluated. Similarly, analogue 4, the enantiomer of tryprostatin B 2 as well as both the diastereomers 6 and 8, were more active than 2 in inhibition of the growth of tumor cells in most of the tumor cell lines evaluated.

5. Experimental

All melting points were determined using a Thomas-Hoover capillary melting point apparatus or an Electrothermal model IA8100 digital melting point apparatus and are uncorrected. Reagents and starting materials were obtained from commercial suppliers and used without further purification unless otherwise indicated. Unless specified otherwise, solvents were freshly distilled prior to use: tetrahydrofuran (THF), benzene, toluene, dioxane, and diethyl ether were distilled under nitrogen from sodium metal utilizing benzophenone as an indicator; MeOH and EtOH were distilled over Mg metal and I_2; dichloromethane was dried over $MgSO_4$ and then distilled over P_2O_5; triethylamine was dried over KOH and then distilled over KOH. Flash column chromatography was carried out on silica gel purchased from E. M. Laboratories (grade 60). HPLC grade solvents were used for all chromatography. Analytical thin-layer chromatography (TLC) was conducted on precoated plates: silica gel 60 F-254, 0.25 mm thickness, manufactured by E. Merck & Co., Germany. Indoles were visualized with Dragendorf's reagent or a saturated solution of ceric ammonium sulfate in 50% H_2SO_4. Ketones or aldehydes